

## Validating the Solar EUV Proxy, $E_{10.7}$

W. Kent Tobiska

SpaceWx/Space Environment Technologies, Los Angeles, CA

**Abstract.** A demonstration of the improvement in thermospheric densities using the daily  $E_{10.7}$  proxy compared to  $F_{10.7}$  is shown. The daily altitude decay for the Solar Mesosphere Explorer (SME) satellite from April 1, 1982 through August 9, 1983, using both proxies and the actual altitude data, are compared. The  $F_{10.7}$  case finished 2 km lower than each of the  $E_{10.7}$  and actual altitude cases which were nearly identical. During active solar conditions, daily  $F_{10.7}$  can overestimate the EUV energy input into the atmosphere by up to 60% and also underestimate it by as much as 50%. Progress is shown towards validating  $E_{10.7}$  as a more accurate proxy compared to  $F_{10.7}$  for use in atmospheric density calculations that are applicable to satellite drag problems. In support of the validation of the  $E_{10.7}$  proxy, an operational prototype hardware/software platform for visualizing of the near-Earth space environment was created. This platform uses a data-driven, data visualization environment. Platform development continues so as to accommodate not only historical data but also nowcast and forecast data streams. Upgrades to the SOLAR2000 Research Grade model are continuing in order to improve the correlation coefficients from multiple linear regressions in several wavelength regions.  $E_{10.7}$  is used in applications that incorporate  $F_{10.7}$ , including empirical thermospheric models, ionospheric models, and general representations of solar activity ranging from climate research to engineering applications.

### 1. Introduction

The requirement for accurate solar extreme ultraviolet (EUV) irradiances, which are a fundamental thermospheric energy input, is driven by the effort to provide self-consistent models of the ionosphere and neutral upper atmosphere. For example, space physics models produce neutral and ionospheric composition, density, and temperature profiles that can be used with operational space systems.

There has been considerable research during the past four decades to measure the variability of solar EUV irradiances or to model them when the data do not exist. It is known that the variations of EUV irradiances are the primary cause for changes in satellite orbital drag, for example. The sources of the solar EUV emission lines and their variability are generally known. The energy from nuclear fusion in the Sun's core is released and transported to the solar visible surface over millions of years by radiative and convective processes in the Sun's interior. This energy manifests itself in thermal and magnetic processes within the solar photosphere, chromosphere, and corona, and gives rise to a highly ionized plasma separated into distinct features governed by the magnetic fields and layers governed by temperature. Radiation is produced throughout the electromagnetic spectrum. The short wavelength emissions are significantly greater than the solar blackbody spectrum or continua emission at EUV wavelengths. They form in the range of higher temperature layers of the outer solar atmosphere such as the chromosphere (>10,000 K), transition region, and cooler (1–2 M K) corona. The emissions are strongly related to magnetic activity of the Sun as seen, for example, in plage regions. Short-term variations, lasting from minutes to hours, are related to eruptive phenomena. Intermediate-term variations on the order of months are modulated by the

27-day rotation period of the Sun and are correlated with the appearance and disappearance of active regions, plage, and network on the solar disk. Long-term variability is related to the 22-year magnetic field cycle of the Sun. *Lean* [1987, 1991], *Rottman* [1987], and *Tobiska* [1993] have reviewed solar EUV variability.

#### 1.1. Proxy representation of the EUV

Because solar spectral EUV is not continuously measured, proxies have been used to represent these emissions. The most common and enduring proxy is the ground-based measured 10.7-cm solar radio emission,  $F_{10.7}$ , which was originally called the Covington index [*Covington*, 1948]. The daily  $F_{10.7}$ , formerly measured and reported at the Algonquin Observatory in Ottawa between February 14, 1947 through May 31, 1991, has more recently been measured with automated equipment at the Penticton, British Columbia observatory starting June 1, 1991. The 2800 megaHertz (10.7 cm) radio intensity consists of emission from three sources including the undisturbed solar surface, developing active regions, and short-lived enhancements above the daily level. The  $F_{10.7}$  levels are measured at local noon (1700 GMT at Ottawa and 2000 GMT at Penticton) and corrected to a few percent for factors including antenna gain, atmospheric absorption, bursts in progress, and background sky temperature (NGDC web site and Ken Tapping, private communication, at the web site <http://www.ngdc.noaa.gov/stp/stp.html>, 2000).

The early connections of  $F_{10.7}$  with EUV irradiances were made in the late 1950's based on observations of 27-day variations in satellite drag and were linked to solar rotational radiation variation in  $F_{10.7}$ . Researchers anticipated that the thermospheric densities actually varied, although it was known at the beginning of the satellite era that  $F_{10.7}$  did not contribute to heating, ionization, nor dissociation processes in the atmosphere. Hence, starting in the late 1950's,  $F_{10.7}$  became a surrogate for solar EUV emissions and has since been used as a standard solar proxy for applications requiring a time-variable representation of upper atmosphere-relevant solar flux. There has been no significant

Copyright 2001 by the American Geophysical Union

Paper number 2000JA000210,  
0148-0227/00/2000JA000210\$09.00

change in the measurement or use of this solar proxy in four decades.

A concept for developing a new EUV proxy was proposed in the 1970's by *Schmidtke* [1976] who suggested that an EUV proxy be formed by summing over wavelength bands. He suggested that a proxy could be developed for specialized applications but could still be based on physical, spectral irradiances. That concept was not revisited in detail until the development of the proxy work described in this paper. Improvements in the empirically modeled EUV spectral irradiances gradually occurred between the late 1970's and 2000 [*Hinteregger*, et al., 1981; *Nusinov*, 1984; *Tobiska*, 1991; *Richards*, et al., 1994; *Tobiska and Eparvier*, 1998; and *Tobiska*, et al., 2000].

However, there was continual resistance among solar proxy users to incorporate these irradiances, much less a new proxy, in place of the traditional  $F_{10.7}$ . This resistance stemmed from several sources. For the 1980's, EUV measurements were nearly non-existent with the exception of USC and LASP rockets that were combined with a brief period of San Marco satellite data. Next, many users had no urgent requirements for substantial improvements in solar EUV spectral irradiances that were different from those obtained a decade earlier. In addition, many empirical models, across many disciplines with many users, had and still have legacy computer code that uses  $F_{10.7}$  as the proxy for solar irradiances. The perception until recently has been that insurmountable code changes would be required to integrate spectral irradiances or a new proxy. Finally, among modelers, it was not well understood what a new proxy would be used for, much less how to design one.

This state of affairs changed in the late 1990's. Following nearly a decade-long, increasing scientific interest in the phenomenon of space weather, i.e., the Sun's radiation and charged particle interactions with the terrestrial environment over human activity time scales, users of space physics models began looking for higher fidelity parameters to represent the space environment. The transitioning of models-for-research to models-for-operations is part of this change. In addition, the drive to improve models comes from government agency programmatic activity to better understand, and represent, space weather. Commercial users of space weather data have additionally refined and elevated their expectations for space weather products. These motivations for general improvements have extended to solar irradiances and occurred at a time when there was a paradigm shift for modelers. It was realized that it is much easier to develop a new irradiance proxy as an input into space physics models than to change the ensemble of legacy code behind the models. In this context, *Schmidtke's* work from a quarter century ago was resurrected.

## 1.2. Development of a new EUV irradiance proxy

Ideally, it was realized that a proxy should completely parameterize the physical quantity it represents and lose no information content. In the case of EUV irradiances, it is suggested that the time-dependent,  $t$ , solar heating of the thermosphere, as a function of EUV energy by wavelength,  $I(\lambda, t)$ , altitudinal heating efficiency,  $\epsilon(\lambda, z)$ , unit optical depth,  $\tau(\lambda, z)$ , absorption cross section of each neutral species,  $\sigma_i(\lambda)$ , and density of each species,  $M_i(z)$ , is the combination of factors that should be represented by a single parameter. Physically, the combination of these quantities is the constituent volume-heating rate in the thermosphere,  $q_i(\lambda, z, t)$  shown in equation 1. Integrated across all species, wavelengths, and altitudes for a unit of time, the total thermospheric heating rate is  $Q(t)$  (equation 2).

$$q_i(\lambda, z, t) = \sigma_i(\lambda) I(\lambda, t) M_i(z) \epsilon(\lambda, z) e^{-\tau(\lambda, z)} \quad (\text{ergs cm}^{-3} \text{s}^{-1}) \quad (1)$$

$$Q(t) = \sum_i \sum_\lambda \sum_z q_i(\lambda, z, t) \quad (\text{ergs s}^{-1}) \quad (2)$$

As a precursor to the derivation of a new proxy using *Schmidtke's* concept, one would want to know what this heating rate actually was for all levels of solar activity. It is possible to calculate a daily heating rate,  $Q(t)$ , for  $i = 1 \dots 8$  neutral thermospheric constituents (O, O<sub>2</sub>, N<sub>2</sub>, CO<sub>2</sub>, NO, He, H, and N), 809 wavelengths for  $\lambda = 1.862$  to 104.9 nm, and  $z = 120 \dots 1000$  km. This heating rate was derived for each day over two solar cycles using a first principles one-dimensional time-dependent (1DTD) thermospheric model [*Tobiska*, 1988; *Tobiska*, et al., 2000]. Since this daily heating rate is a physical quantity convolving all the solar components relevant to thermospheric heating, it was useful to find a single proxy that parameterizes the heating rate since it is rather complex to calculate.

This daily heating rate,  $Q(t)$ , was compared with a simpler approximation, i.e., the solar EUV energy,  $I(\lambda, t)$  ( $\text{ergs cm}^{-2} \text{s}^{-1} \Delta\lambda^{-1}$ ), integrated between 1.862 – 104.9 nm at the top of the Earth's atmosphere,  $E(t)$ . *Tobiska*, et al. [2000] found only minor differences at the 1-2% level when these two quantities were compared after  $E(t)$  was translated into units of  $Q(t)$  by linear regression. Because of the good comparison and the simpler calculation,  $E(t)$  has been adopted as the basis for the new proxy and can be written as equation 3. The translation to the units of  $F_{10.7}$  is accomplished by a linear regression technique relating  $E(t)$  to  $F_{10.7}$  between July 1, 1977 and June 30, 1999. The regression coefficients are then used to create the pseudo- $F_{10.7}$  or the equivalent  $E_{10.7}$  (equation 4). This third degree polynomial that creates the  $E_{10.7}$  proxy results in a correlation coefficient of 0.957 for the  $E(t) - F_{10.7}$  regression. The high correlation stems from the high correspondence of long-term, solar cycle variation although there can be significant daily differences. The term  $E_{10.7}$  indicates that the proxy is the total EUV energy arriving at the top of the Earth's atmosphere reported in the same units as the historical  $F_{10.7}$  proxy. The SOLAR2000 Research Grade empirical model (S2K) [*Tobiska*, et al., 2000; *Tobiska*, 2000] produces variable EUV irradiances, including the  $E_{10.7}$  time-dependent solar EUV proxy.

$$E(t) = \sum_\lambda I(\lambda, t) \quad (\text{ergs cm}^{-2} \text{s}^{-1}) \quad (3)$$

$$F_{10.7} \approx E_{10.7} = a_0 + a_1 E(t) + a_2 E(t)^2 + a_3 E(t)^3 \quad (\times 10^{-22} \text{ W m}^{-2} \text{ Hz}^{-1}) \quad (4)$$

The validation of  $E_{10.7}$  magnitude and variability was accomplished using two tests [*Tobiska*, et al., 2000]. The first test compared standard deviations from several least-square fits for a variety of proxy derivations and selected the formulation in equations 3 and 4 as the best fit to  $Q(t)$ . The intent of that exercise was to compare variations based on the physics of the atmosphere to the empirical variations of the solar flux obtained from a simple integration, i.e., the theory and a simple proxy formulation were compared and found to be consistent with each other in daily variability.

The second test of *Tobiska*, et al. [2000] compared monthly mean  $E_{10.7}$  and  $F_{10.7}$  when both were used to calculate satellite orbit decay. It was found that in all the longer-term physical solar variations, such as the 11-year solar cycle and months-long active region growth-decay,  $E_{10.7}$  is nearly identical to  $F_{10.7}$ . The intent of the second exercise was to provide confidence in the new proxy, i.e., going beyond the theory-formulation comparison to show the general case where the new proxy is nearly the same as the old proxy for longer time scale variations.

*Tobiska*, et al., [2000] provided confidence for both the theory-formulation comparison and similarities between monthly

mean  $E_{10.7}$  and  $F_{10.7}$ . In the third validation exercise reported here, it is important to show the differences between the two proxies for their daily values (see subsection 2.2 Satellite Drag) and to describe what those differences mean in the context of improved solar irradiance specification. The following discussion is the third in a series of on going validation exercises for  $E_{10.7}$ .

## 2. Discussion

### 2.1. Rationale, applications, and availability of $E_{10.7}$

The  $E_{10.7}$  proxy is particularly useful for satisfying operational space system requirements related to space weather information. It has the capability for providing a temporal solar input to the near-Earth space environment. This capability exists because  $E_{10.7}$  can be generated from historical, nowcast, and/or forecast solar EUV irradiances. Prior to describing specific applications of  $E_{10.7}$ , it is important to describe why space weather information and forecasting technologies are receiving attention. The following description provides the rationale for developing  $E_{10.7}$ .

The energy, transportation, and communication industries that form three significant economic pillars of our society are examples of sectors that have grown through remarkable technological advances. This growth during the past half century is partially driven by microelectronic advances and increasing utilization of space. With these new technologies, however, our society has experienced new types of risks. Hazards originate from the very environment that has helped create these new technologies, i.e., from the Sun and from near-Earth space.

Space weather risks to these new technologies are growing due to space-related, technology-related, and geo-political-related trends. It is possible to mitigate these risks. The space-related trends that are influencing the growth in risk to these industries are based on the following conditions of:

- an increased understanding of the physical processes that create space weather which has led to a perception of “nothing can be done” to “we must do something” (basic research is transitioned into commercial applications);
- an increased spacecraft launch rate and an increased use of low-Earth space (four-fold increase in last 5 years);
- an increase in debris and collision probabilities (more satellites, more debris);
- the proposed use of the lower thermosphere for suborbital space plane flights (90-150 km);
- the stringent requirements for launch trajectories and impact limit lines, in the event of launch failure, and for spacecraft de-orbit capability without endangering populations or entering sovereign airspace;
- an increased agency funding profile for monitoring the space environment (e.g., in the U.S., the NASA Living With a Star initiative, the NSF space weather funding, the National Space Weather Program, and the National Polar Orbiting Environmental Satellite System program);
- an increased public awareness of the phenomena of space weather (greater publicity); and
- the suggestion of increasingly severe space weather (turbulence and/or instabilities in the lower thermosphere).

The technology-related trends influencing the growth in risk to these industries are based on the following conditions of:

- the increased reliance upon space-based technologies, e.g., telecommunications requiring large volumes of data transfer (more cell-phone, video, and data exchange activity);
- an increased requirement for current and future information in all commercial sectors (continuing trend);

- an increased reliance on internet/intranet information exchange (expanding infrastructure);
- a desire for no interruption of telecommunications services under any space weather conditions (continues current trend);
- an increase in restrictions on telecommunications frequencies at specific locations so as to accommodate more users and more bandwidth (continues current trend);
- an increase in pointing precision and location knowledge requirements (restricted future real estate in space means precise pointing requirements);
- an increased susceptibility of our technology to solar-terrestrial events (new technologies introduce new risks);
- the emergence of faster computers enabling more rapid and complex calculations (Moore’s Law implies that speed translates into enhanced computing/modeling capability);
- a desire for a reduction of technological risks (implies higher profit margins and is a continuing trend); and
- an increase in customers who want information regardless of what they decide to do with it.

The geo-political-related trends influencing the growth in risk to these industries are based on the following conditions of:

- an increased commercial globalization (extrapolation of an ongoing, multi-decade trend); and
- a continued instability in the world political arena that mandates greater security capabilities (continued threats from small wars and terrorism imply greater demand for immediate, on-demand, and accurate information).

In order to mitigate space hazards and their risks, there are a number of identified applications of  $E_{10.7}$  that serve different users. Table 1 outlines the types of users and their needs for which  $E_{10.7}$  provides a service. These users include, but are not limited to, government agencies, LEO constellation satellite operators, GEO communication satellite operators, satellite manufacturers, insurance companies, commercial airlines, space-plane manufacturers, GPS providers, and cell-phone service providers.

$E_{10.7}$  is developed for availability in historical, nowcast, and forecast time categories as described in detail by *Tobiska*, et al. [2000] and *Tobiska* [2000]. A summary of these categories, time frames, the first release status and SOLAR2000 version that produces  $E_{10.7}$ , the applications types, and the availability dates are outlined in Table 2.

The SOLAR2000 Research Grade v1.05 model that first produced  $E_{10.7}$  was released in September 2000 as an IDL® application with a graphical user interface (GUI). It is available in newer versions for download to researchers at the SpaceWx web site. A sample listing of the output of the model is shown in Table 3 for the 7-day period of July 25 - July 31, 1999. This was a period of high solar activity that included numerous flares toward the second half of that 7-day period.

Table 3 presents the ASCII tabular listing format of the SOLAR2000 output product by the research grade model. It contains a metadata section as well as time-tagged solar data. Three time formats are listed as YYYY-DDD, calendar, and Julian day. Solar data is listed as  $F_{10.7}$ , 81-day  $F_{10.7}$ , Lyman-alpha, 81-day Lyman-alpha,  $E_{10.7}$ , 81-day  $E_{10.7}$  and the integrated solar spectrum,  $S(t)$ , that is only variable in short wavelengths from 1-122 nm in versions 1.yz The output file has a fixed format and the  $E_{10.7}$  proxy can be read easily from a unique field in each time record (row). There is one record for each time step. In the case of historical data prior to the current epoch, there is one record per day. For nowcast data covering the time frame of the current 24-hour epoch, the operational grade version of the model produces several records per day including 3-hourly and, eventually, mi-

**Table 1.** User types and their needs

User needs	User types
1) risk assessment and probabilities (quantify risks and conduct post-analysis studies)	1) government agencies, LEO constellation satellite operators, GEO communication satellite operators, satellite manufacturers, insurance companies, commercial airlines, space-plane manufacturers
2) system requirement specification (validate requirements with historical data sets)	2) government agencies, LEO constellation satellite operators, GEO communication satellite operators, satellite manufacturers, insurance companies, commercial airlines, space-plane manufacturers
3) monitoring service (provide alerts, warnings, and user-specific displays)	3) government agencies, public institutions, GPS providers, LEO constellation satellite operators, GEO communication satellite operators, commercial airlines, cell phone operators
4) near real time TEC uncertainty maps (mitigate GPS signal uncertainty resulting from solar activity, irregularities, and scintillation)	4) government agencies, GPS providers, LEO constellation satellite operators, GEO communication satellite operators, satellite manufacturers, commercial airlines, cell phone operators
5) high time resolution solar irradiance specification (minutes to hours)	5) government agencies, GPS providers, LEO constellation satellite operators, GEO communication satellite operators, commercial airlines, cell phone operators
6) near-term and long-term forecasts solar irradiance specification (hours to days and months to years)	6) government agencies, GPS providers, LEO constellation satellite operators, GEO communication satellite operators, commercial airlines, cell phone operators
7) ionospheric height specification (specify and forecast RF link paths and probabilities)	7) government agencies, GPS providers, LEO constellation satellite operators, GEO communication satellite operators, satellite manufacturers, commercial airlines, space plane manufacturers, cell phone operators
8) high precision location knowledge (reduce object orbit/re-entry location uncertainties)	8) government agencies, LEO constellation satellite operators, GEO communication satellite operators, cell phone operators
9) high precision pointing capability (reduce object targeting uncertainty)	9) government agencies, LEO constellation satellite operators, GEO communication satellite operators, cell phone operators
10) debris avoidance capability (reduce uncertainty)	10) government agencies, space plane manufacturers
11) near-Earth space plane flight control and trajectory corridor information (improve flight control and vehicle trajectory safety/efficiency)	11) government agencies, commercial airlines, space plane manufacturers
12) interplanetary environment specification (long-term mission planning)	12) government agencies, satellite manufacturers

nutely time resolution. Forecast data beyond the current epoch is produced with 3-hourly or daily time resolution depending upon how distant into the future the forecast is made.  $E_{10.7}$  is operationally available on all these time resolutions and categories.

Figure 1 demonstrates the graphical output of the SOLAR2000 research grade model for a broad time frame including the July, 1999 7-day period described above. In this example, a subset of the input data and results are shown in Table 3. The integrated solar spectrum,  $S(t)$ ,  $F_{10.7}$ , and Lyman-alpha are the 3 panels of the first row. In the second row, the full 1-nm solar spectrum from 1-1,000,000 nm and the 1 nm EUV spectrum from 1 – 122 nm are shown in SI units of  $W m^{-2}$ . It should be noted that although the ASTM E490 spectrum used by SOLAR2000 v1.yz at each wavelength longward of Lyman-alpha does not contain measured data at 1 nm resolution beyond approximately 2000 nm, the solar

blackbody emission is interpolated to provide those values. In the third row, the comparison between  $F_{10.7}$  and  $E_{10.7}$  is plotted for a user-selected data period.

## 2.2. Satellite Drag

A rationale for going beyond the  $F_{10.7}$  proxy in the development of the  $E_{10.7}$  proxy rests with the fact that contemporary space system operations require greater precision and accuracy in spacecraft attitude and orbit determination. The current state-of-the-art capabilities have 15% uncertainties (J. Owens and F. Marcos, private communications, 2000). This represents the limit of  $F_{10.7}$  proxy capability and it is not able to provide the next level of improvement. While  $F_{10.7}$  continues to serve a wide variety of users, its limitations are not surprising since it has no physical connection to the upper atmosphere, it only marginally represents so-

**Table 2.** E<sub>10.7</sub> applications and availability

Categories	Time frame	First release status	Application types	Availability date
Historical	Feb 14, 1947 to near the current epoch	<b>SOLAR2000 v1.05 and v1.15:</b> released as a research grade models at SpaceWx	Post analysis: <ul style="list-style-type: none"> <li>• anomaly resolution</li> <li>• trend analysis</li> </ul>	September 2000 (v1.05) and January 2001 (v1.15)
Nowcast	the current epoch (24-hours with minutely, 3-hourly, and daily time resolution)	<b>SOLAR2000 v1.15:</b> released as an operational grade model at NOAA/SEC (CRADA product for daily nowcast) and at SpaceWx (high time resolution)	Real-time operations: <ul style="list-style-type: none"> <li>• vehicle reentry</li> <li>• next-orbit maneuvers</li> <li>• docking events</li> </ul>	April 2001 (v1.15)
Forecast	current epoch to solar cycle (3-hourly to daily time resolution) <ul style="list-style-type: none"> <li>• 1-72 hours</li> <li>• 3-14 days</li> <li>• 14-28 days</li> <li>• 1-6 months</li> <li>• 1/2-11 years</li> <li>• 1-5 solar cycles</li> </ul>	<b>SOLAR2000 v1.15:</b> released as operational grade commercial grade models at SpaceWx for high time resolution and forecast capability	Scheduling/planning: <ul style="list-style-type: none"> <li>• operational staffing and schedules</li> <li>• extra-project resource negotiation and scheduling</li> <li>• satellite communication link estimation</li> <li>• lifetime estimation</li> <li>• mission requirement specifications</li> <li>• planetary gravity assists, maneuvering, and aerobraking</li> </ul>	April 2001 (v1.15)

lar EUV irradiances, and it will not capture temporal changes of less than a day.

In this third validation activity for E<sub>10.7</sub> as a solar proxy, an extension of the second test reported by Tobiska et al. [2000] is described below. That test compared both F<sub>10.7</sub> and E<sub>10.7</sub> monthly means when they were used as inputs to a Long-term Orbit Propagator (LOP) to generate satellite altitude decay profiles [Tobiska, 1988]. LOP, coupled with a Jacchia-71 (J71) thermospheric model, used daily F<sub>10.7</sub> or E<sub>10.7</sub> values interpolated from monthly averages to determine a density at each satellite altitude. The case of the Solar Mesosphere Explorer (SME) was examined where SME was in a sun-synchronous orbit at approximately 540-km altitude starting in 1981. Actual SME ephemeris altitude data for a year and a half were compared with LOP predicted altitudes using the monthly average F<sub>10.7</sub> or E<sub>10.7</sub> values. That study found a nearly identical behavior between the F<sub>10.7</sub> and E<sub>10.7</sub> modeled orbits for SME. The orbit prediction started on March 31, 1982 (1982-090) and ended on October 1, 1983 (1983-274). At the end, there was only 200-300 meters difference between the actual and predicted altitudes referenced to a

mean equatorial radius of the Earth of 6378.164 km based on monthly averaged proxies.

The activity reported here demonstrates improvement in thermospheric density estimation using daily E<sub>10.7</sub> compared to daily F<sub>10.7</sub>. The daily altitude decay for SME, using both daily proxies compared to the actual satellite altitude data, was studied with the LOP program. The run period was from April 1, 1982 through August 9, 1983. Daily E<sub>10.7</sub> and F<sub>10.7</sub> were input into the J71 model that has been coded as a subroutine of LOP. Both cases started the orbit integrator at 6909.06 km and ran for 495 days during the decline of solar cycle 21. The classical orbit elements of SME at the start time are shown in Table 4.

At the end of the run, on August 9, 1983, the actual mean SME altitude was 519.302 km above the mean Earth equatorial radius, the E<sub>10.7</sub> case was 519.244 km, and the F<sub>10.7</sub> case was 517.242 km. The input proxies and the resultant altitudes of SME can be seen in Figure 2. From this figure's top panel, the F<sub>10.7</sub> overestimates the EUV energy input into the atmosphere by up to 60% and also underestimates it by as much as 50% on a daily basis during active solar conditions. In doing so, the Figure 2 bot-

**Table 3.** Sample SOLAR2000 output file

```

SOLAR2000 RESEARCH GRADE V1.05 Output file
Run date: 30-Oct-2000 11:37:48.00
METADATA:
Days in this file: 7
Units: wavelengths (nm), SI (W m-2), photon flux (photons cm-2 s-1), energy flux (ergs cm-2 s-1)
Dates and proxies (E81 is 81-day average valid for time series > 81 days across selected range):
YYYY-DDD      calendar      Julian day  F10.7  F81  Ly-a  Ly-81  E10.7  E81  s
1999-206/12:00:00  25-JUL-1999/12:00:00  2451385.00000  188.0  173.4  4.96E+11  4.77E+11  173.1  161.9  1367.28090
1999-207/12:00:00  26-JUL-1999/12:00:00  2451386.00000  177.8  173.0  5.03E+11  4.77E+11  169.1  161.7  1367.28093
1999-208/12:00:00  27-JUL-1999/12:00:00  2451387.00000  179.9  172.6  5.11E+11  4.77E+11  169.9  161.4  1367.28108
1999-209/12:00:00  28-JUL-1999/12:00:00  2451388.00000  203.9  172.2  5.15E+11  4.77E+11  178.8  161.2  1367.28133
1999-210/12:00:00  29-JUL-1999/12:00:00  2451389.00000  208.6  171.7  5.15E+11  4.76E+11  180.2  160.9  1367.28136
1999-211/12:00:00  30-JUL-1999/12:00:00  2451390.00000  212.2  171.3  5.22E+11  4.76E+11  181.5  160.7  1367.28151
1999-212/12:00:00  31-JUL-1999/12:00:00  2451391.00000  206.7  170.7  5.16E+11  4.76E+11  178.9  160.4  1367.28135
    
```

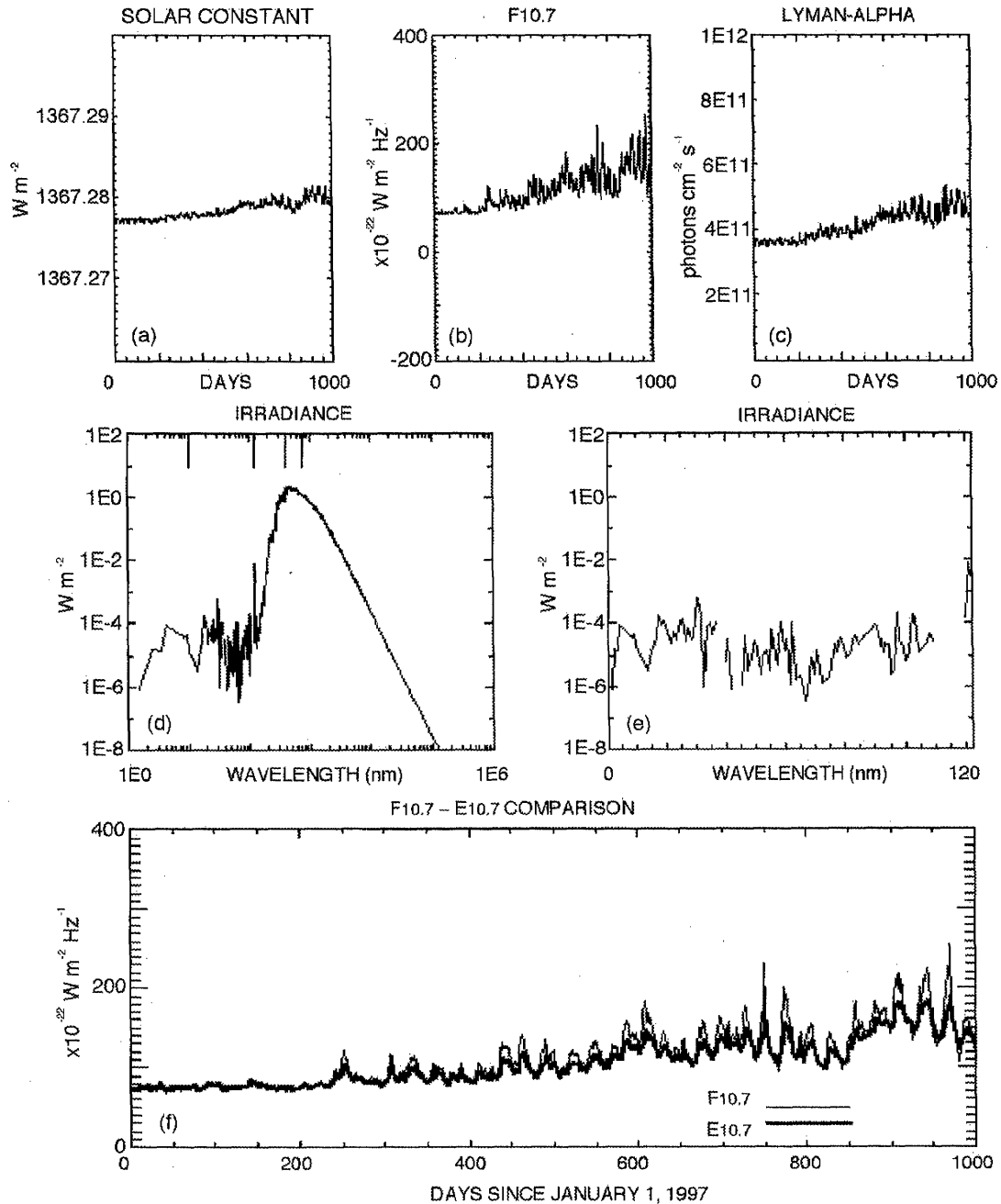


**Figure 1.** Sample output of the SOLAR2000 Research Grade v1.05 model for 1000 days starting January 1, 1997. This format provides quick-look information for a user including the  $E_{10.7}$  proxy. Panels in the top row (a, b, c) show the solar constant,  $F_{10.7}$ , and Lyman-alpha for the example time period. In version 3.yz, the solar constant,  $S(t)$ , is the same as the variable total solar irradiance (TSI). However, in version 1.yz, only the 1-122 nm range is variable in the integrated solar spectrum. Panels in the second row (d and e) show the full solar spectrum at 1 nm resolution and the variable EUV wavelengths shortward of Lyman-alpha on the first day of the model run. The panel in the third row (f) shows the comparison between  $E_{10.7}$  (dark line) and  $F_{10.7}$  (light line) for the example time period.

**Table 4.** SME classical orbit elements on April 1, 1982

Classical Elements	a	e	i	$\Omega$	$\omega$	MA
Units	km	-	deg	deg	deg	deg
Values	6909.0599	0.0010000	97.616000	358.25221	90.243847	142.24466

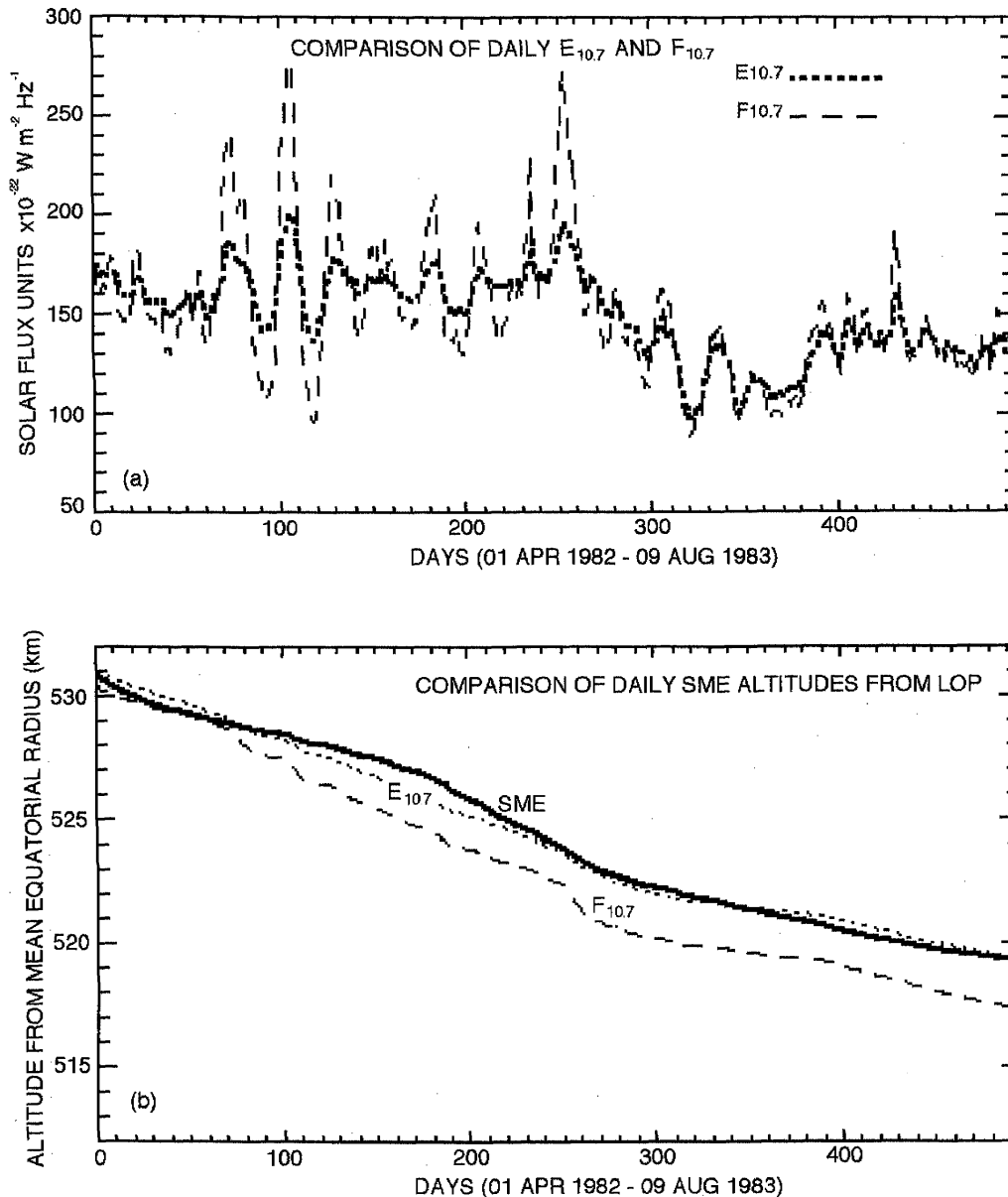


**Figure 2.** The top panel (a) shows the comparison between  $E_{10.7}$  and  $F_{10.7}$  for the period of April 1, 1982 through August 9, 1983.  $F_{10.7}$  varies much more than  $E_{10.7}$  and produces an overestimate of the EUV heating of the atmosphere. The bottom panel (b) demonstrates that excess  $F_{10.7}$  causes the J71 model and the orbit propagator to overestimate the drag on SME. This results in unrecoverable orbit altitude error compared to the SME ephemeris data. On the other hand,  $E_{10.7}$  used in the J71 atmosphere and orbit propagator captures nearly all the solar variability.

tom panel demonstrates that the excess EUV heating of the atmosphere estimated by  $F_{10.7}$  causes the J71 model and the orbit propagator to overestimate the drag on SME. This results in unrecoverable orbit altitude error during the run. On the other hand, the  $E_{10.7}$  estimate for EUV heating and subsequent atmospheric drag is nearly identical to the actual SME case. These results provide the validation of  $E_{10.7}$  as the more accurate solar proxy for atmospheric density calculations that are applicable to satellite drag problems when compared to  $F_{10.7}$ . The validation activity has linked solar, thermospheric density, and orbit propagator models to represent an entire physical system.

$E_{10.7}$  is designed to be used as a direct replacement in any application that uses  $F_{10.7}$ , including empirical thermospheric models, ionospheric models, and general representations of solar activity ranging from climate research to engineering applications. There are five advantages of using  $E_{10.7}$  versus  $F_{10.7}$  and they range from data availability to representations of physical processes.

- Historical:  $E_{10.7}$ , as produced by SOLAR2000, will upgrade its historical accuracy using data from new missions such as TIMED, ISS Solar Platform, and GOES. The historical accuracy of  $F_{10.7}$  will remain static.

